Chapter

Investigation on Internal Short Circuit Identification of Lithium-Ion Battery Based on Mean-Difference Model and Recursive Least Square Algorithm

Xu Zhang, Yue Pan, Enhua Wang, Minggao Ouyang, Languang Lu, Xuebing Han, Guoqing Jin, Anjian Zhou and Huiqian Yang

Abstract

Electric vehicles powered by lithium-ion batteries take advantages for urban transportation. However, the safety of lithium-ion battery needs to be improved. Self-induced internal short circuit of lithium-ion batteries is a serious problem which may cause battery thermal runaway. Accurate and fast identification of internal short circuit is critical, while difficult for lithium-ion battery management system. In this study, the influences of the parameters of significance test on the performance of an algorithm for internal short circuit identification are evaluated experimentally. The designed identification is based on the mean-difference model and the recursive least square algorithm. First, the identification method is presented. Then, two characteristic parameters are determined. Subsequently, the parameters of the significance calculation are optimized based on the measured data. Finally, the effectiveness of the method for the early stage internal short circuit detection is studied by an equivalent experiment. The results indicate that the detection time can be shortened significantly via a proper configuration of the parameters for the significance test.

Keywords: lithium-ion battery, internal short circuit identification, significance test, mean-difference model, equivalent experiment

1. Introduction

Safety and energy saving as well as environmental protection are the key points for automobile industry development [1, 2]. Lithium-ion batteries have been widely used due to their high energy density, long cycle life, low environmental pollution, no memory effect, and high charge and discharge rates [3–5]. With the rapid development of materials technology, the energy density of lithium-ion batteries is gradually increased, causing the thermal runaway events accordingly. Its safety

problem must be taken into account seriously [6–9]. The safety of batteries may affect the confidence of the users of electric vehicles. Therefore, battery safety is one of the biggest obstacles for the application of electric vehicles. Internal short circuit is an important step leading to the thermal runaway. Thus an accurate and rapid identification for internal short circuit is necessary and needs to be solved [10].

The internal short circuit can be detected by comparing the output of the battery with a threshold or a predicted value via a mathematical model. Ikeuchi et al. measured the electricity output of the battery and compared with a threshold computed by the ampere-hour integration [11]. Ouyang et al. proposed three characteristic parameters according to the parameter effect and the depleting effect of an internal short-circuited battery. The variations of the open circuit voltage (OCV) and the internal resistance were determined based on a mean-difference model. Then, a significance criterion and a fault tolerance mechanism were used to judge whether the internal short circuit happened [12]. Feng et al. used a 3D electrochemical-thermal model to simulate the internal short circuit and regarded it as a parameter estimation problem [13]. The measured voltage and the temperature of the cell were input to a model to evaluated excessive depletion of the capacity and abnormal heat generation. The internal short circuit resistance was estimated by Seo et al. according to the SOC variation and the discrete ampere-hour integrals from an equivalent circuit model with internal short circuit branches [14]. Xia et al. employed a voltage correlation coefficient and a threshold to determine whether an internal short circuit occurred via capturing the initial abnormal voltage signal [15]. This method could eliminate the influence of the SOC. Zhang et al. designed a low-pass filter to estimate the leakage current and the resistance of the internal short circuit cell in real time [16]. Kang et al. developed a multi-fault diagnostic strategy based on an interleaved voltage measurement topology. An improved correlation coefficient method was employed to eliminate the inconsistency among the cells and the measurement errors [17]. Kong et al. used a principle of similar charging voltage to obtain the remaining charging electricity and used the average voltage to obtain the internal short circuit resistance and thus the internal short circuit was identified. However, the charging voltage does not have similarities in some cases, and the average voltage may not be correctly obtained [18]. Feng et al. analyzed the characteristics of internal short circuit using an electrochemical-thermal coupling model. This is significant for internal short circuit identification, but it also reveals the difficulty of internal short circuit identification [19].

The operation conditions of the lithium-ion battery in an electric vehicle are very complicated and its safety is critical. Therefore, it is important to find a method which can detect the self-induced internal short circuit in time. Our previous study proposed a method to detect the internal short circuit [12]. However, the detection time of this method is still not satisfactory. In this study, the identification method for the internal short circuit is modified, and the influences of the parameters of the significance test are evaluated. Then, the modified identification algorithm is validated via an equivalent experiment. First, the basic working principle and procedures for the internal short circuit detection are introduced based on the mean-difference model. Then, the parameters for the internal short circuit identification are configured. Next, a replacement experiment is carried out, and the results of this method are computed. Subsequently, the results of a significance test are analyzed. The outcomes indicate that the detection time can be shortened significantly compared with those of the previous study. Finally, the possibility of the identification algorithm for early-stage internal short circuit detection is investigated. The results of this study can provide a reference for the practical applications so that the safety of lithium-ion batteries can be improved.

2. Identification method

The mathematical model of the designed identification method is presented in this section. First, the equivalent circuit model is introduced. Then, the mean-difference model and the recursive least square algorithm are described. Finally, the identification procedure is illuminated.

2.1 Equivalent circuit model

Figure 1(a) shows the equivalent circuit model of a lithium-ion battery with an internal short circuit resistor, where R_{ISCr} and I_{ISCr} are the resistance and the current of the internal short circuit, respectively:

Based on **Figure 1(a)**, the OCV can be expressed by

$$U = \frac{R_{ISCr}}{R + R_{ISCr}} E - \frac{R_{ISCr}}{R + R_{ISCr}} RI. \tag{1}$$

When the internal short circuit resistance approaches infinite, it can be taken as there is no internal short circuit. However, if it is less than a certain value, an internal short circuit branch may be considered to be generated in the battery cell. The parameter effect is the change of internal resistance and open circuit voltage due to the internal short circuit branch according to Eq. (1). The depleting effect is the drop of the open circuit voltage and the fluctuation of the internal resistance caused by the self-discharge of the internal short circuit battery.

2.2 Mean-difference model

The parameters of the equivalent circuit model for different cells inside a battery pack are not the same due to the discrepancies of material ingredients, manufacturing processes, and working conditions. The mean-difference model includes a mean model for the pack and a difference model for each cell, which can be used to represent difference among the cells. The parameters of the mean model are obtained according to the average performance of the battery pack. Meanwhile, the difference model displayed in **Figure 1(b)** describes the difference of a specific cell against the mean model. In **Figure 1(b)**, ΔU_i, ΔE_i, and ΔR_i are the differences between the i-th cell and the mean model of the battery pack. For a battery pack in series connection, the current flowing through each cell is uniform.

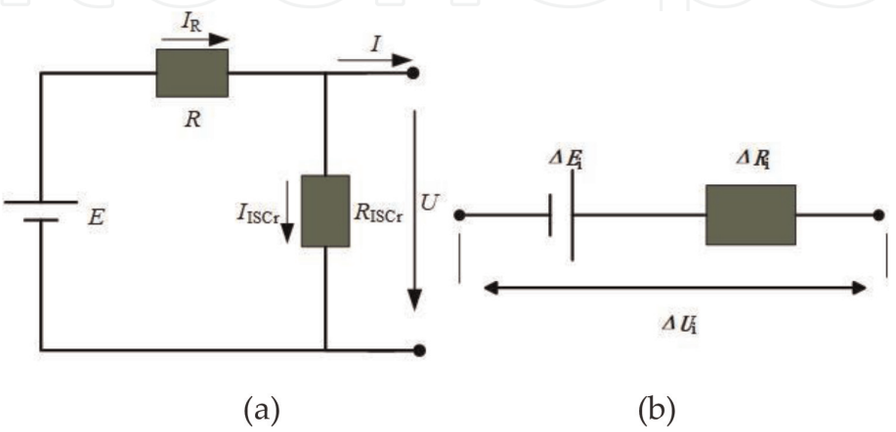

Figure 1.
Equivalent circuit of lithium-ion battery: (a) circuit with internal short circuit resistor and (b) mean-difference model of a cell.

U_{mean} is the average cell voltage calculated by excluding the highest and lowest voltages among these cells.

2.3 Recursive least square algorithm

For a battery pack in series layout, the total current and the terminal voltage can be measured. Accordingly, U_{mean} and ΔU_i can be calculated by Eqs. (2) and (3):

$$\Delta U_i = \Delta E_i - I\Delta R_i \tag{2}$$

$$\Delta U = U_i - U_{mean} \tag{3}$$

After that, ΔE_i and ΔR_i can be identified by the recursive least square (RLS) algorithm with a forgetting factor, which is represented by Eqs. (4)–(7). In this algorithm, ΔE_i and ΔR_i are the parameters needed to be identified, and φ is the recursor:

$$Y = \Delta U_i \tag{4}$$

$$Y = \varphi \bullet \theta \tag{5}$$

$$\theta = (\Delta E_i, \Delta R_i)^T \tag{6}$$

$$\varphi = (1, -I) \tag{7}$$

The calculation process of the RLS algorithm with a forgetting factor can be expressed by Eqs. (8)–(12):

$$y(k) = \varphi(k)\theta(k) + e(k) \tag{8}$$

$$e(k) = y(k) - \varphi(k)\hat{\theta}(k-1) \tag{9}$$

$$K(k) = \frac{P(k-1)\varphi^T(k)}{\lambda + \varphi(k)P(k-1)\varphi^T(k)} \tag{10}$$

$$P(k) = \frac{P(k-1) - K(k)\varphi(k)P(k-1)}{\lambda} \tag{11}$$

$$\hat{\theta}(k) = \hat{\theta}(k-1) + K(k)e(k) \tag{12}$$

where $y(k)$ is the system output, $\varphi(k)$ is the vector that can be measured, $\theta(k)$ is the vector to be estimated, $P(k)$ is the covariance matrix, $K(k)$ is the gain, and λ is the forgetting factor.

2.4 Identification procedure

The variations of ΔE_i and ΔR_i are due to the parameter effect and the depleting effect as well as the inconsistencies among all the cells of the battery pack. The characteristic parameters that can be used to identify the internal short circuit should reflect the difference between the internal short circuit cell and the others and can be represented by the mean-difference model. At the same time, the battery SOC and the internal short circuit resistance have great influences on the internal short circuit identification [20]. There is a one-to-one correspondence between the SOC and the OCV. As a result, ΔE can reflect the discharge capacity of the battery, which relates to the situations of the internal electrochemical reaction of the battery. $fluc(\Delta R)$ is the fluctuation of the computed internal short circuit resistance in a certain interval and can be used to label the event of the internal short circuit of the battery cell. In our previous investigation, three different

parameters including ΔE_i, $d(\Delta E_i)/dt$ and $fluc(\Delta R_i)$ were used to detect the internal short circuit independently [12]. However, the performance of this method for the early-stage internal short circuit detection was not satisfied. Therefore, a modified method taking into account both ΔE_i and $fluc(\Delta R_i)$ is designed in this study.

The main decision process is described in **Figure 2**. First, the terminal voltage and the operation current of the i-th cell are measured, and the average terminal voltage is calculated. Then, ΔU_i can be determined by the mean-difference model. Next, the parameters ΔE_i and ΔR_i are identified by the RLS method. According to the parameter effect and the depleting effect, the value of ΔE_i of the internal short circuit battery is always negative, while the value of ΔR_i fluctuates up and down. Then, the internal short circuit is judged by a significance calculation. In this study, to improve the accuracy of identification, an anti-false alarm mechanism is adopted; if 80% of 150 continuous data range of the significance calculation results exceed a prescribed threshold, an event of internal short circuit is setup by the characteristic parameter. Only these two characteristic parameters (ΔE_i and $fluc(\Delta R_i)$) detect the event of internal short circuit simultaneously; a final decision of the internal short circuit is confirmed. This anti-false alarm mechanism is a modification based on the previous method in [12].

The forgetting factor λ affects the stability of the least squares algorithm. The stability of the algorithm increases as the λ approaches 1. However, the identification precision for the actual parameter variation diminishes. When λ decreases, the calculated results may diverge. An optimal range of λ is obtained as 0.99–0.995 based on the test results with different internal short circuit resistances. To keep the error as small as possible, especially for the value of ΔR_i, while maintaining the RLS algorithm stable, the forgetting factor is set to 0.992 in this study.

In the previous method [12], $d(\Delta E_i)/dt$ was also used to identify the internal short circuit. In this study, it is found that $d(\Delta E_i)/dt$ is not reliable due to limitations of the sampling frequency and the sampling accuracy and is not recommended. ΔE_i and ΔR_i are directly obtained by the identification algorithm. The fluctuation value $fluc(\Delta R_i)$ of the internal resistance is obtained as the standard deviation of 150 continuous sampling points adjacent to the current moment, which is expressed by

$$fluc(\Delta R(kT)) = StDev\{\Delta R((k-149)T), \Delta R((k-148)T), ..., \Delta R(kT)\}. \quad (13)$$

where *StDev* is the standard deviation. Significance calculation results are obtained according to the extreme values of characteristic parameters, the average value μ, and the standard deviation σ. The μ and σ are calculated by removing the

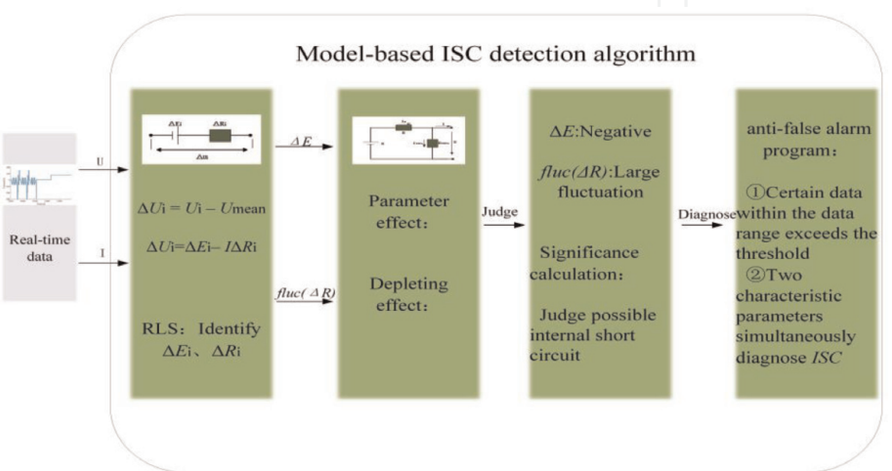

Figure 2.
Detection procedure for internal short circuit.

extreme values of the characteristic parameters. The positive and negative significances can be represented by

$$M_{pos}(x) = \frac{x_{max} - \mu}{\sigma}, \tag{14}$$

$$M_{neg}(x) = \frac{x_{min} - \mu}{\sigma}. \tag{15}$$

After that, the threshold is set to ±3. We can consider the significance calculation in this way: the extent of the extreme value deviating from the average value μ of the characteristic parameters by the number of σ.

3. Results and discussion

The nickel-cobalt-manganese (NCM) ternary lithium-ion battery is used for this experiment. The battery module is a parallel connection of three batteries and then connected in series. The layout of the battery cells on the test rig is shown in **Figure 3(a)**. The cell has a capacity of 50 Ah. The identification algorithm treats these three parallel groups as one series group with each cell having a capacity of 150 Ah. The equivalent resistance replacement method is employed to simulate the

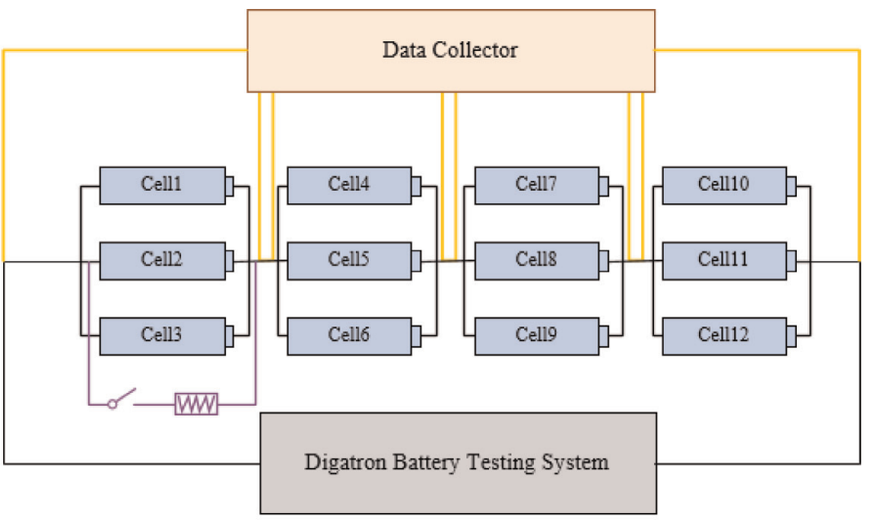

(a)

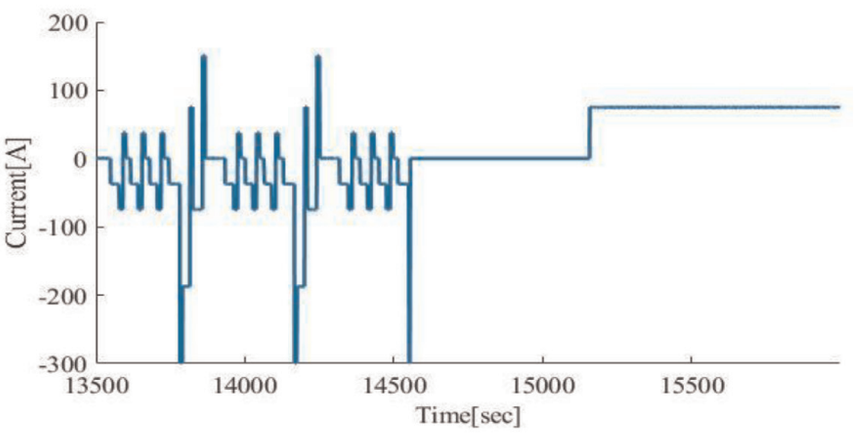

(b)

Figure 3.
Configurations for the equivalent experiments: (a) layout of the battery module and (b) DST test cycle for the load configuration.

electrical characteristics of the internal short circuit battery. The dynamic stress test (DST) cycle is used as an input. The DST working condition is shown in **Figure 3(b)**, which can represent typical state changes of the battery under the practical operation conditions of electric vehicles. A data collector is used to measure the current and voltage of each cell. The accuracies for the current and voltage measurement are 0.1%, and the sampling frequency is set to 1 Hz. The maximum charge/discharge rate of the DST cycle is set to 2C. When the minimum cell voltage decreases to 2.75 V, the DST test is terminated. After 10 min rest, the battery pack is charged with a constant current of 75 A (0.5C) until the voltage of any cell reaches 4.2 V. After resting for another 10 min, the next cycle is proceeded again.

An equivalent resistor with a precision of 0.1% is used in the experiment. The internal short circuit can be triggered or cancelled via a switch. In this experiment, three different values for the internal short circuit resistance are used including 1, 10, and 100 Ω, respectively. The results of the three resistances are used to validate the identification algorithm and compared with those of the previous method [12]. The terminal voltage and the current of each cell are measured and inputted to the internal short circuit identification algorithm programed in MATLAB.

3.1 Experimental results

The results of the modified identification method are given in **Figures 4–6** for an external resistor of 1, 10, and 100 Ω, respectively. First, the measure values of

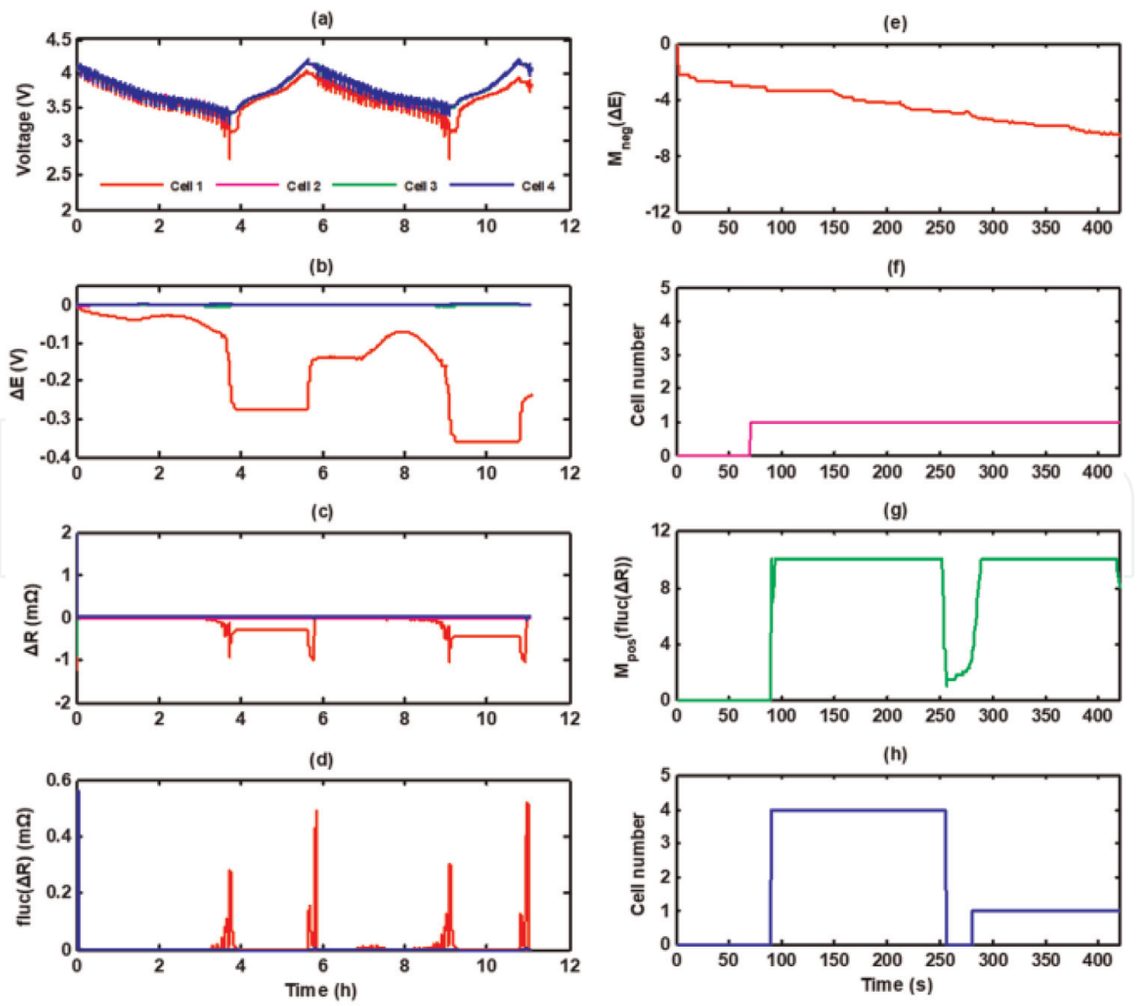

Figure 4.
Results of the equivalent experiment with an external resistor of 1 Ω: (a) the measured terminal voltage, (b) ΔE_i, (c) ΔR_i, (d) $fluc(\Delta R_i)$, (e) the negative significance of ΔE, (f) the relative cell number of $M_{neg}(\Delta E)$, (g) the positive significance of $fluc(\Delta R)$, (h) the relative cell number of $M_{pos}(fluc(\Delta R))$.

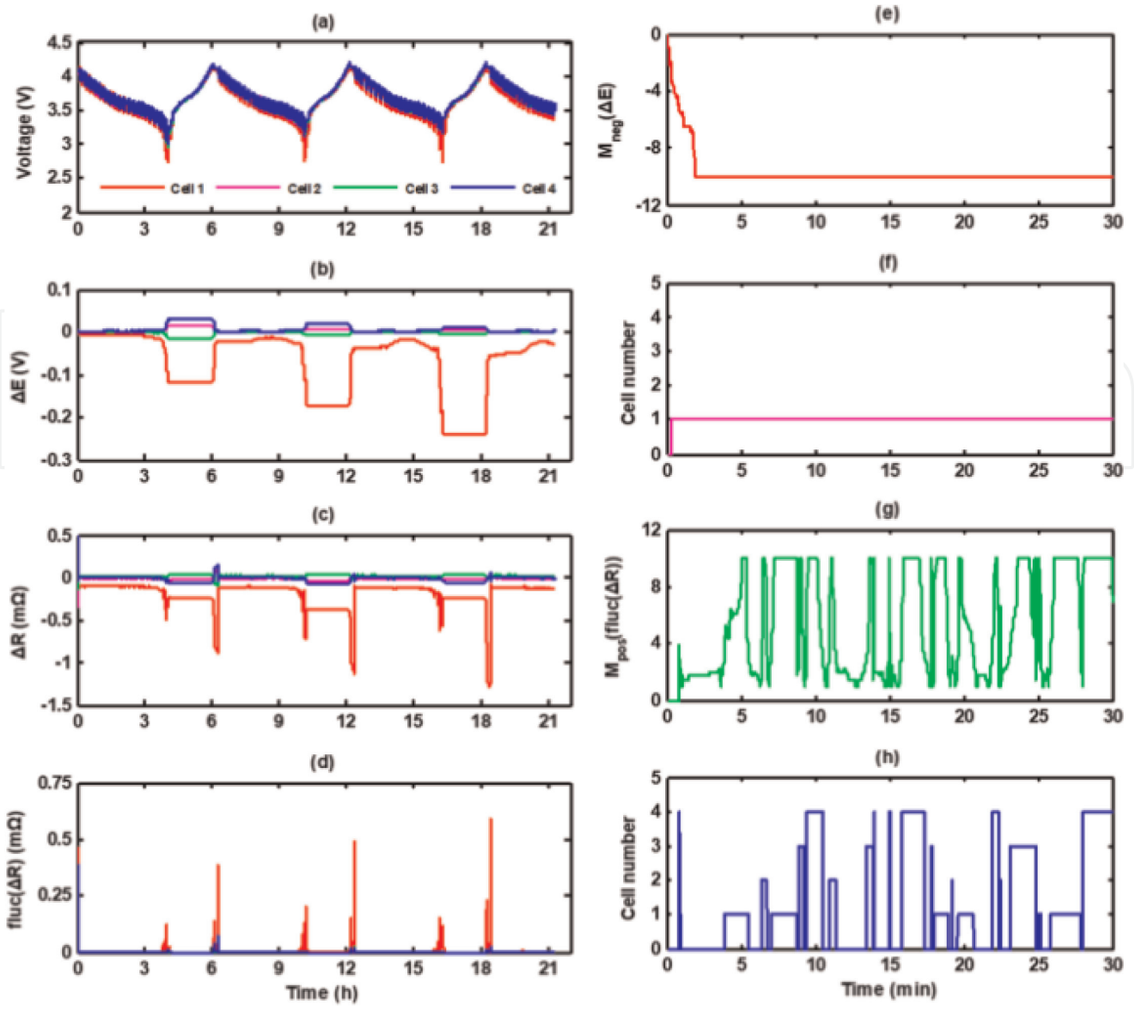

Figure 5.
Results of the equivalent experiment with an external resistor of 10 Ω: (a) the measured terminal voltage, (b) ΔE_i, (c) ΔR_i, (d) $fluc(\Delta R_i)$, (e) the negative significance of ΔE, (f) the relative cell number of $M_{neg}(\Delta E)$, (g) the positive significance of $fluc(\Delta R)$, (h) the relative cell number of $M_{pos}(fluc(\Delta R))$.

the terminal voltage are displayed. Then, ΔE_i and ΔR_i for each cell are determined by the mean-difference model and the RLS algorithm. Later, $fluc(\Delta R_i)$ is computed based on the values of ΔR_i and Eq. (13). It can be seen that the discharge power with an internal short circuit resistor of 1 Ω is the largest, resulting in a greatest influence on the terminal voltage of the cell and the fluctuation of ΔR_i.

For each case, the internal short circuit cell (i.e. Cell 1) already reaches the lowest voltage after the first DST cycle, leading to a much lower SOC. When the SOC drops to a very low value, the OCV is more sensitive. Therefore, a sudden drop of ΔE_i occurs at the end of the discharging process. The voltage of the short circuit cell recovers slightly after 10 min rest. Then, the battery pack undergoes a constant-current charging. The polarization internal resistance of the battery increases during this process, and the overvoltage rises for all the cells. The voltage for each cell decreases to a stable value gradually after another 10 min rest.

The change rate of ΔR_i increases at the end of the DST cycle owing to a low SOC state. At this moment, the cell has experienced a deep discharging process, and a large part of the lithium ions enter into the porous electrode. Effects of the electrochemical polarization and the concentration polarization weaken, leading to a sudden decrease of ΔR_i. The results of ΔR_i keep constant during the constant-current charging process in this method. When the discharging begins again, it returns to its actual value.

The results for the detection time are listed in **Table 1** and compared with those in [12]. It can be seen that the detection time of the modified identification method is much shorter than the previous one. The reason is mainly attributed to the judge criteria being relaxed. To prevent the occurrence of false alarm, both the conditions for ΔE_i and $fluc(\Delta R_i)$ are adopted simultaneously. The results indicate that the performance of the previous method for the internal short circuit detection can be improved significantly via this modification.

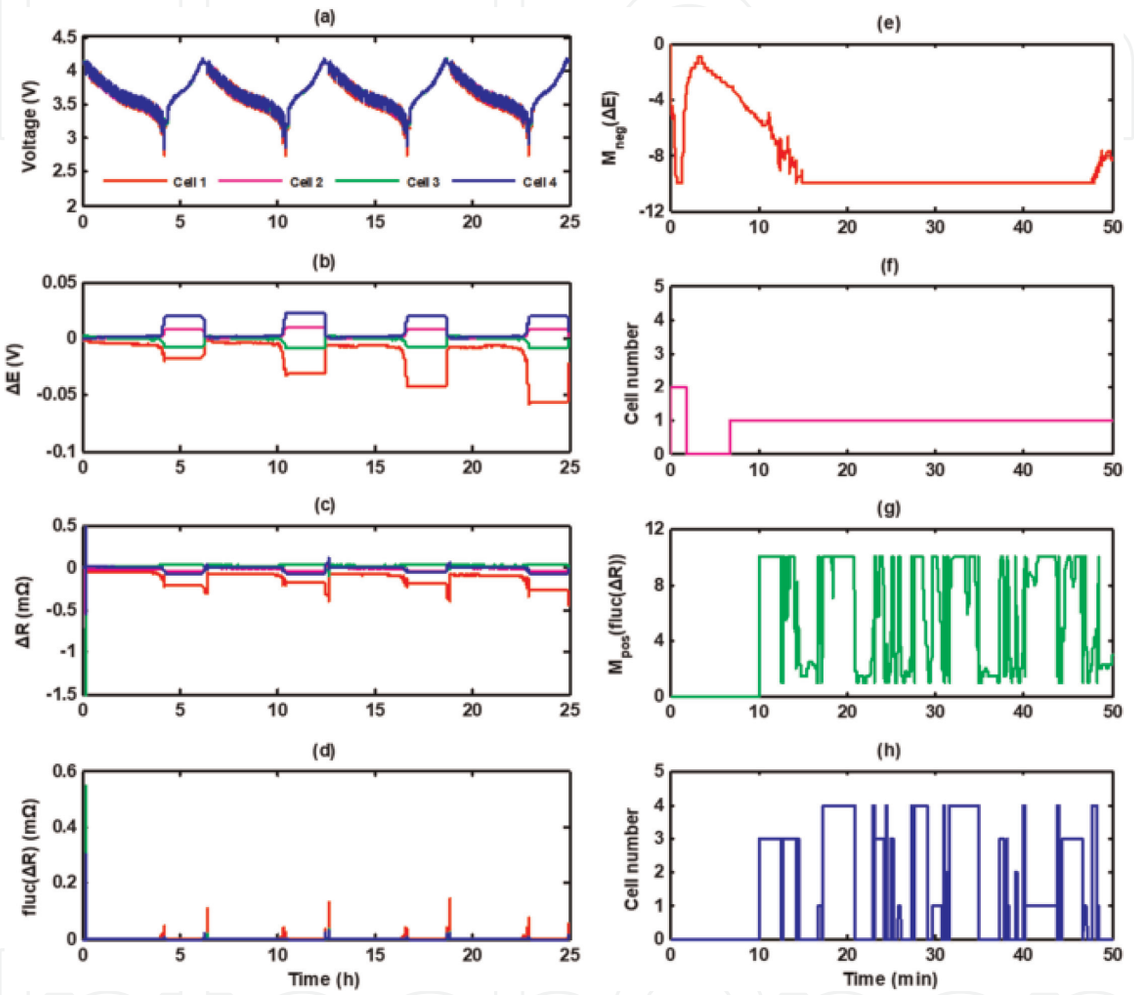

Figure 6.
Results of the equivalent experiment with an external resistor of 100 Ω: (a) the measured terminal voltage, (b) ΔE_i, (c) ΔR_i, (d) $fluc(\Delta R_i)$, (e) the negative significance of ΔE, (f) the relative cell number of $M_{neg}(\Delta E)$, (g) the positive significance of $fluc(\Delta R)$, (h) the relative cell number of $M_{pos}(fluc(\Delta R))$.

Parameter	Criteria	100 Ω	10 Ω	1 Ω
ΔE_i & $fluc(\Delta R_i)$[a]	$(M_{neg}(\Delta E_i) < -3)$ & $(M_{pos}(fluc(\Delta R_i)) > 3)$	42 min	27 min	6 min40 s
ΔE_i[b]	$M_{neg}(\Delta E_i) < -6$	11 h 19 min	1 h 18 min	24 min
$fluc(\Delta R_i)$[b]	$M_{pos}(fluc(\Delta R_i)) > 10$	4 h 43 min	1 h 17 min	22 min
Improvement (%)[c]		85.2%	64.9%	69.7%

[a] *Results of this study.*
[b] *Results of the previous method [12].*
[c] *Improvement of a relative to b.*

Table 1.
Experimental results and comparison with the previous method.

3.2 Analysis of significance test

The results of the significance calculation for an external resistor of 1 Ω are shown in the right column of **Figure 4**. The significance value for ΔE_i is given in **Figure 4(e)**, and the corresponding cell number is labelled in **Figure 4(f)**. The significance of ΔE_i is negative due to the influences of the parameter and depleting effects. If the significance value is higher than −3, no cell number is labelled, and a value of 0 is specified. The significance value for $fluc(\Delta R_i)$ is positive and shown in **Figure 4(g)**. The significance value of $fluc(\Delta R_i)$ is limited by a maximum value of 12 to give a clear exhibition. The results of the corresponding cell number are displayed in **Figure 4(h)**. To enhance the reliability of this method, the anti-false alarm program (80% of the significant values among a continuous 150 points for both ΔE_i and $fluc(\Delta R_i)$ exceed the thresholds) is employed to confirm an event of the internal short circuit finally. In this experiment, the external resistor is connected by switching it on at the very beginning. The event of the internal short circuit is detected at the time of 400 s. The results of the significance test for 10 and 100 Ω are given in **Figures 5** and **6**, respectively. Likewise, a minimum of −12 is set if the negative significance is less than −12. The significance value of ΔE_i can identify the right short circuit cell quickly. However, the results of $fluc(\Delta R_i)$ vary dramatically and will take much longer to give the right outcome.

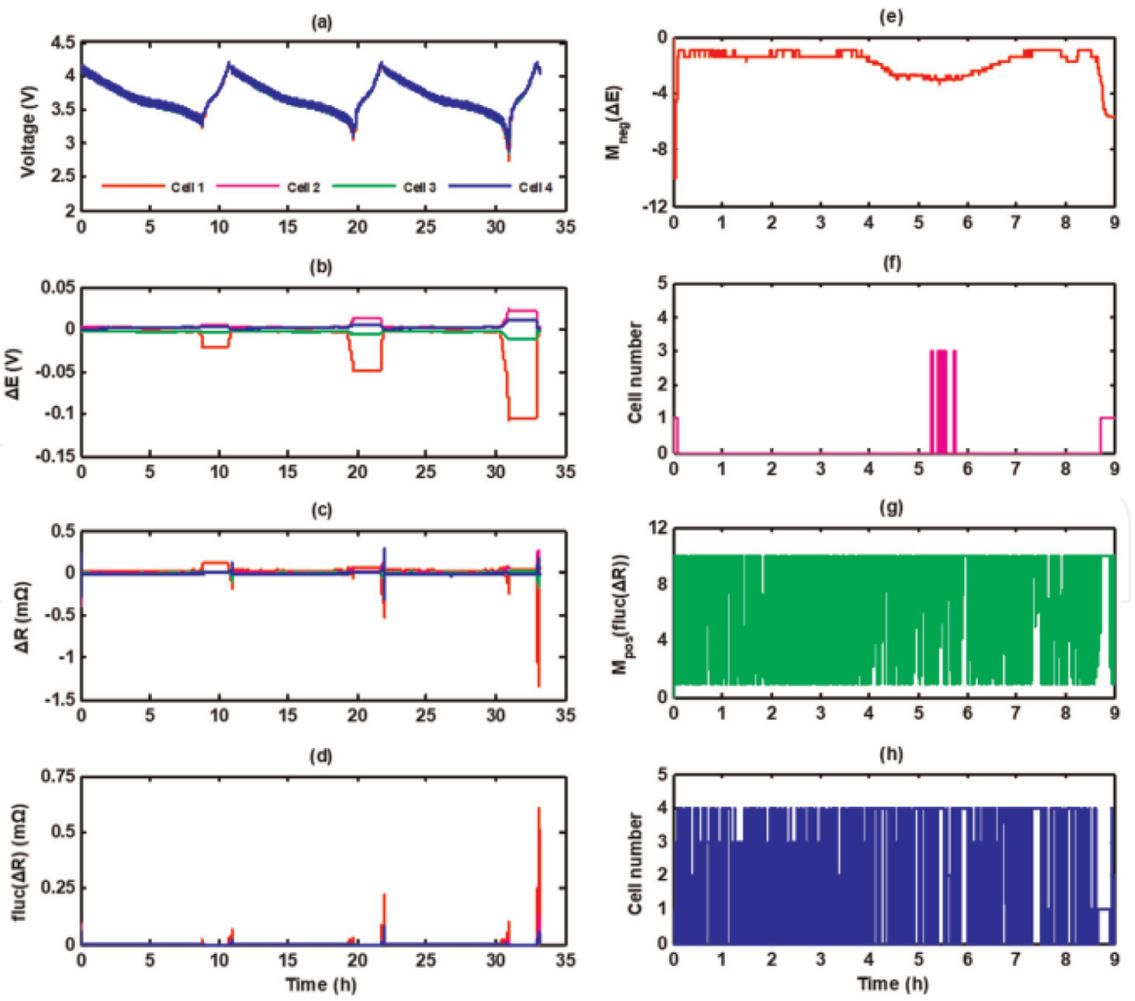

Figure 7.
Results of the equivalent experiment with an external resistor of 1000 Ω: (a) the measured terminal voltage, (b) ΔE_i, (c) ΔR_i, (d) $fluc(\Delta R_i)$, (e) the negative significance of ΔE, (f) the relative cell number of $M_{neg}(\Delta E)$, (g) the positive significance of $fluc(\Delta R)$, (h) the relative cell number of $M_{pos}(fluc(\Delta R))$ [21].

3.3 Results for early stage identification

If an internal short circuit can be detected at the beginning, protection measures can be adopted in time, and the system safety can be improved significantly. However, when a self-induced internal short circuit emerges at the early stage, the ISR resistance is very large. Accordingly, the variations of the OCV and the ISR current are very small. The possibility of this method for the early-stage internal short circuit identification is studied in this section [21]. An external resistance of 1000 Ω with a 0.1% precision is used in this equivalent experiment. The results are shown in **Figure 7**. Because the variation magnitudes of ΔE_i and $fluc(\Delta R_i)$ are much smaller, the identification method cannot identify the internal short circuit by the significance test under the normal SOC range. If the SOC drops to a very low value, where the slope of OCV versus SOC is increased and the internal short circuit can be identified. After 8 h and 40 min, the internal short circuit is detected for the case of 1000 Ω.

3.4 Discussion

The algorithm is based on the mean-difference model. There is a certain deviation in this model. In addition, the internal short circuit itself also generates noises for the identification algorithm. These may cause the internal resistance of the battery fluctuating more than other normal batteries. The true internal short circuit should be produced by the internal electrochemical reaction and the growth and change of the internal dendrites. At the same time, the temperature change caused by the internal short circuit will affect the electrochemical structure inside the battery, so the resistance fluctuation of the actual internal short circuit battery is larger than that of the normal battery. The external resistance used in the simulation of the internal short circuit may be different from the actual internal short circuit, but the equivalent experiment method still can be used to simulate the electrical characteristics of the internal short circuit battery. The battery resistance fluctuation of the equivalent experiment is smaller than the resistance fluctuation of the actual internal short circuit battery. As the internal short circuit battery ages, the lithium-ion and active materials in the battery decrease. The internal short circuit resistance of the battery fluctuates more, and the open circuit voltage will also drop faster.

The problem of internal short circuit detection caused by inconsistency is tricky, especially for the characteristic parameter of ΔE. However, the evolution of the internal short circuit is a cumulative process. It is only possible to have an internal short circuit at a specific time and in a specific working condition. Generally, the internal short circuit occurs in a battery with poor consistency. Even if the internal short circuit occurs on a battery with a relatively high voltage, the internal short circuit will continuously self-discharge. The internal short circuit can be correctly recognized with the help of the characteristic parameter of $fluc(\Delta R)$, although the time may become longer.

In the case of extreme SOC, the algorithm is limited by the inherent characteristics of the battery itself, and the internal short-circuited battery may be affected by the inconsistency, the polarization, and the solid-phase diffusion in the battery electrode particles at the extreme low SOC, causing the algorithm to produce a possible misjudgment. However, in electric vehicles, the working range of the battery generally would not reach the extreme SOC, so the algorithm can be used for internal short circuit identification in the normal driving range.

For the identification of early internal short circuit, it is difficult to separate the difference between internal short circuit and self-discharge. The voltage

characteristics of self-discharge and internal short circuit are consistent. The threshold cannot be set to completely distinguish between self-discharge and internal short circuit. Therefore, early internal short circuit identification is easy to be misreported.

4. Conclusions

In this chapter, an identification method is presented for the internal short circuit of lithium-ion battery based on the mean-difference model and the recursive least square algorithm with a forgetting factor. This method is a modification of our previous investigation. The working principle and test procedure are described at first. Then, its performance is compared with that of the previous method. Subsequently, the influence of the parameters of the significance test on the detection time is analyzed. Finally, the possibility of this method for the early-stage internal short circuit identification is estimated.

The criteria of the significance test for the internal short circuit detection are adjusted, and two characteristic parameters (ΔE_i and $fluc(\Delta R_i)$) are employed to identify the internal short circuit simultaneously. Meanwhile, an anti-false alarm program is added to improve its reliability. Compared with the results of the previous study, the detection time can be shortened significantly by 64–85% via configuring the parameters of the significance test properly.

Because the self-induced internal short circuit resistance is very large at the early stage, this method cannot detect the internal short circuit event when the SOC is in the range of normal operation conditions. However, if the self-induced internal short circuit resistance reduces close to 100 Ω, the internal short circuit event can be identified successfully by this method, which can be integrated into the battery management system to monitor the operation of lithium-ion battery within the normal working range. A warning signal can be specified if an internal short circuit is detected so that the security of electric vehicles can be improved.

Acknowledgements

The authors would like to thank for the support of the National Natural Science Foundation of China (Grant No. U1564205 and 51876009), the Beijing Natural Science Foundation (Grant No. 3184052), and the Cooperation Project of Chongqing Changan New Energy Vehicle Technology Co., Ltd (No. 1811420009).

Conflict of interest

The authors declare no conflict of interest.

Abbreviations

DST	dynamic stress test
ISC	internal short circuit
NCM	nickel-cobalt-manganese
OCV	open circuit voltage
RLS	recursive least square
SOC	state of charge

Author details

Xu Zhang[1], Yue Pan[2], Enhua Wang[1*], Minggao Ouyang[2], Languang Lu[2], Xuebing Han[2], Guoqing Jin[3], Anjian Zhou[3] and Huiqian Yang[3]

1 School of Mechanical Engineering, Beijing Institute of Technology, Beijing, China

2 State Key Laboratory of Automotive Safety and Energy, Tsinghua University, Beijing, China

3 Chongqing Changan New Energy Vehicle Technology Co., Ltd, Chongqing, China

*Address all correspondence to: enhua.wang@yahoo.com

References

[1] Mehigan L, Deane JP, Gallachoir BP, Bertsch V. A review of the role of distributed generation (DG) in future electricity systems. Energy. 2018;**163**: 822-836

[2] Wang Q, Li S, Li R. China's dependency on foreign oil will exceed 80% by 2030: Developing a novel NMGM-ARIMA to forecast China's foreign oil dependence from two dimensions. Energy. 2018;**163**:151-167

[3] Li M, Xu H, Li W, Liu Y, Li F, Hu Y. The structure and control method of hybrid power source for electric vehicle. Energy. 2016;**112**:1273-1285

[4] Uddin K, Jackson T, Widanage WD, Chouchelamane G, Jennings PA, Marco J. On the possibility of extending the lifetime of lithium-ion batteries through optimal V2G facilitated by an integrated vehicle and smart-grid system. Energy. 2017;**133**:710-722

[5] Smiley A, Plett GL. An adaptive physics-based reduced-order model of an aged lithium-ion cell, selected using an interacting multiple model Kalman filter. Journal of Energy Storage. 2018; **19**:120-134

[6] Kvasha A, Gutierrez C, Osa U, de Meatza I, Blazquez JA, Macicior H. A comparative study of thermal runaway of commercial lithium ion cells. Energy. 2018;**159**:547-557

[7] Chen K, Zheng F, Jiang J, Zhang W, Jiang Y, Chen K. Practical failure recognition model of lithium-ion batteries based on partial charging process. Energy. 2017;**138**:1199-1208

[8] Berrueta A, Urtasun A, Ursúa A, Sanchis P. A comprehensive model for lithiumion batteries: From the physical principles to an electrical model. Energy. 2018;**144**:286-300

[9] Fu Y, Lu S, Shi L, Cheng X, Zhang H. Ignition and combustion characteristics of lithium ion batteries under low atmospheric pressure. Energy. 2018;**161**: 38-45

[10] Williard N, He W, Hendricks C, Pecht M. Lessons learned from the 787 dreamliner issue on lithium-ion battery reliability. Energies. 2013;**6**:4682-4695

[11] Ikeuchi A, Majima Y, Nakano I. Circuit and method for determining internal short-circuit, battery pack, and portable device. US20140184235A1; 2014

[12] Ouyang M, Zhang M, Feng X, Lu L, Li J, He X, et al. Internal short circuit detection for battery pack using equivalent parameter and consistency method. Journal of Power Sources. 2015; **294**:272-283

[13] Feng X, Weng C, Ouyang M, Sun J. Online internal short circuit detection for a large format lithium-ion battery. Applied Energy. 2016;**161**:168-180

[14] Seo M, Goh T, Park M, Koo G, Kim SW. Detection of internal short circuit in lithium-ion battery using model-based switching model method. Energies. 2017;**10**:76

[15] Xia B, Shang Y, Nguyen T, Mi C. A correlation based detection method for internal short circuit in battery packs. In: 2017 IEEE Applied Power Electronics Conference and Exposition (APEC). 26–30 March 2017; Tampa, FL, USA

[16] Zhang Z, Kong X, Zheng Y, Zhou L, Lai X. Real-time diagnosis of micro-short circuit for Li-ion batteries utilizing low-pass filters. Energy. 2019;**166**: 1013-1024

[17] Kang Y, Duan B, Zhou Z, Shang Y, Zhang C. A multi-fault diagnostic

method based on an interleaved voltage measurement topology for series connected battery packs. Journal of Power Sources. 2019;**417**:132-144

[18] Kong X, Zheng Y, Ouyang M, Lu L, Li J, Zhang Z. Fault diagnosis and quantitative analysis of micro-short circuits for lithium-ion batteries in battery packs. Journal of Power Sources. 2018;**395**:358-368

[19] Feng X, He X, Lu L, Ouyang M. Analysis on the fault features for internal short circuit detection using an electrochemical-thermal coupled model. Journal of the Electrochemical Society. 2018;**165**:A155-A167

[20] Liu B, Jia Y, Li J, Yin S, Yuan C, Hu Z, et al. Safety issues caused by internal short circuits in lithium-ion batteries. Journal of Materials Chemistry A. 2018;**6**:21475-21484

[21] Zhang X, Pan Y, Wang E, Ouyang M. Investigation on early-stage internal short circuit identification for power battery pack. Advances in Engineering Research. 2019;**184**:233-235